

# Life Estimation of a Composite Structural Component in a Multi-Axial Stress State

C. Colombo<sup>1</sup> and L. Vergani<sup>1</sup>

<sup>1</sup> Politecnico di Milano, Dipartimento di Meccanica  
Via La Masa 1, 20156 Milano, ITALY  
e-mail: chiara.colombo@mecc.polimi.it; laura.vergani@polimi

**ABSTRACT.** *Aim of this work is to test and understand the mechanical behaviour, in multi-axial stress condition, of a composite material used to build a structural component, a corner beam of bus cabin. The bus cabin design is part of the European project Litebus, whose aim is the design of a module of a lightweight coach.*

*A series of experimental tests was performed on specimens cut out from this beam. Different fibers orientation with respect to the direction of load application were considered: longitudinal (0°), normal (90°), inclined at 30° and 45°. The static and fatigue characterization were carried out to identify the mechanical behaviour in terms of S-N curves. Obtained fatigue data are then interpolated by fitting parameters required for multi-axial models of fatigue life estimation.*

## 1. INTRODUCTION

The European project “*Litebus*” [1] aims to develop a modul of a coach whose main characteristic is the reduction in weight. In this project, *Politecnico di Milano* is involved in the durability study of the components: one of the studied elements of the bus cabin is a pultruded corner profile placed along the motion direction of the coach. It is made of E-glass reinforce fibers and vinyl-ester matrix. The glass fiber content is 50%, of which more than a half (30% of the total composite volume) is in the longitudinal direction, as indicated by the manufacturer.

This component, during its life, is generally loaded by fatigue multi-axial loadings. So, in order to obtain an optimal structural design it is necessary to estimate its multi-axial fatigue life. The problem is complex: the fatigue multi-axial criteria are, in fact, not deeply known when applied to composite materials.

In literature [2-5] there are, basically, two kinds of approaches: the micro and the macro-approach. The first one is related to the possible failure modes depending on detailed local failure development, such as fibre breakage, interface debonding and matrix cracking or yielding.

In the second approach the failure is described by means of macroscopic criteria, generally in terms of average stress to which the composites are subjected.

Other criteria can be classified as macroscopic approaches, but based on the local observed failure modes [6, 7].

It is important to put in evidence [8] that the multi-axial stress condition in the composite structures is due to a combination of external loadings, and local stress states, due to the material anisotropy. In the large-scale composite structures with complex shapes, in fact, the fiber orientation spatially varies and the composite elements are locally subjected to off-axis loading. Thus, even if the loading is uni-axial the local stress state is multi-axial.

The fatigue damage mechanisms depend on the local stress fields, even the external multi-axial loading effect can be reduced to a change of the local stress states.

Thus, the fatigue criteria based on local stress fields seem to be more effective than the ones formulated considering the global coordinates.

The aim of this paper is, therefore, to estimate the fatigue life of a complex component, by considering the local different failure modes in presence of off-axis loadings. Specimens have been extracted from the beam along the fibers direction, in the transversal in-plane one, in  $30^\circ$  and  $45^\circ$  direction with respect to the fibers' axis. Static and fatigue tests were carried out to obtain the fatigue curves and all the mechanical parameters useful to apply the criteria and to estimate the component fatigue life.

## 2. STATIC AND FATIGUE CHARACTERIZATION OF THE COMPOSITE

Four sets of rectangular specimens are cut off from the beam:  $L$ , with the fibers along the longitudinal direction,  $N$ , with the fibers along the normal direction,  $I(30^\circ)$  and  $I(45^\circ)$ , respectively with fibers inclined at  $30^\circ$  and  $45^\circ$ .

The static characterization of the pultruded material is performed by the testing machine MTS Alliance RF/150 and by the extensometer MTS 63431 F-24 (base length: 25 mm); crosshead speed is set to 2 mm/mm. During the tests, the elastic modulus  $E$  and the ultimate strength  $\sigma_u$  are measured. The results of the static tests are summarized in Tab. 1, together with the number of tested specimens. Confidence bands are calculated by means of the *t-student* statistic, considering a probability of 95%.

The failure modes of the considered specimens are different: examples of broken samples representing the analyzed types are shown in Fig. 1. It is possible to notice that the  $L$  specimen (Fig. 1.a) broke due to an interface fiber-matrix delamination and fiber rupture. For the  $N$  specimen shown in Fig. 1.b, fibers lay perpendicularly to the load and the static strength is offered only by the matrix properties. A similar behavior is shown for the  $I$  specimens of Fig. 1.c and 1.d. The fibers are cut and offer only partially mechanical strength to the composite. Most of the load is underwent by the matrix. This consideration is supported by the results of the static tests reported in Tab. 1: it is evident the huge difference in terms of ultimate strength between the  $L$  specimens and the  $N$  and  $I$  ones, for which the fibers are cut.

From Tab. 1 it is also possible to observe that the variance in the results is smaller for the  $L$  and  $I(45^\circ)$  specimens, while the highest data dispersion is shown by the  $N$  specimens. This high data dispersion is essentially due to the large number of defects

and imperfections present in the resin, which is characterized, in consequence, by a large spread of the strength values. The high dispersion of  $I(30^\circ)$  is due to the small specimens' number.

Table 1. Results of the static tests.

Tested specimens	Specimen set			
	$L(0^\circ)$	$N(90^\circ)$	$I(45^\circ)$	$I(30^\circ)$
E [MPa]	11662±1437	3910±1163	7700±974	7941±2275
$\sigma_u$ [MPa]	145.2±31.5	42.7±6.9	69.4±8.4	73.5±18

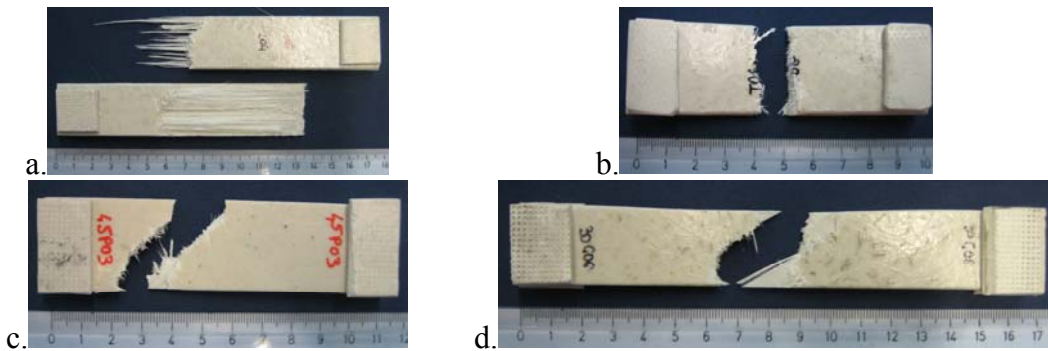


Figure 1. Typical failures occurred during static tests for L (a.), N (b.),  $I(45^\circ)$  (c.) and  $I(30^\circ)$  (d.) specimens.

Fatigue tests are carried out on the MTS-810 uni-axial testing machine. Tests are performed at constant frequency (20 Hz) and considering a fixed stress ratio ( $R=0.1$ ). Test is considered run-out at  $5 \cdot 10^6$  cycles.

The results of the tests are summarized in Fig. 2. From these plots it is possible to observe that the  $N$  specimens show high data dispersion, as in the static tests, while  $L$  and  $I$  specimens have almost the same statistical dispersion.

Failure modes of fatigue specimens are similar to the ones shown in Fig. 1 for the static tests.

### 3. CRITICAL DISCUSSION

The linear regression of the  $\sigma_{\max} - \log N$  plot (corresponding to the Wöhler diagram) can be expressed in the semi-log scale as:

$$\sigma_{\max} = \alpha_0 + \beta_0 \cdot \log N \quad (1)$$

A second criterion used to interpolate the fatigue data is indicated in [9] and based on the equations by [10]. The basis equation is:

$$\sigma_u - \sigma_{\max} = \alpha_1 \left( \frac{\sigma_{\max}}{\sigma_u} \right)^{0,6 - \psi |\sin \theta|} \left[ \sigma_{\max} (1 - \psi)^{1,6 - \psi |\sin \theta|} \right] \frac{1}{f^{\beta_1}} (N^{\beta_1 - 1}) \quad (2)$$

where  $\sigma_u$  is the average strength obtained from static tests,  $\sigma_{\max}$  is maximum stress applied during loading,  $\psi$  corresponds to the stress ratio  $R$  for uni-axial fatigue tests,  $f$  is the frequency and  $\theta$  is the angle between the fibers and the axis of load application.

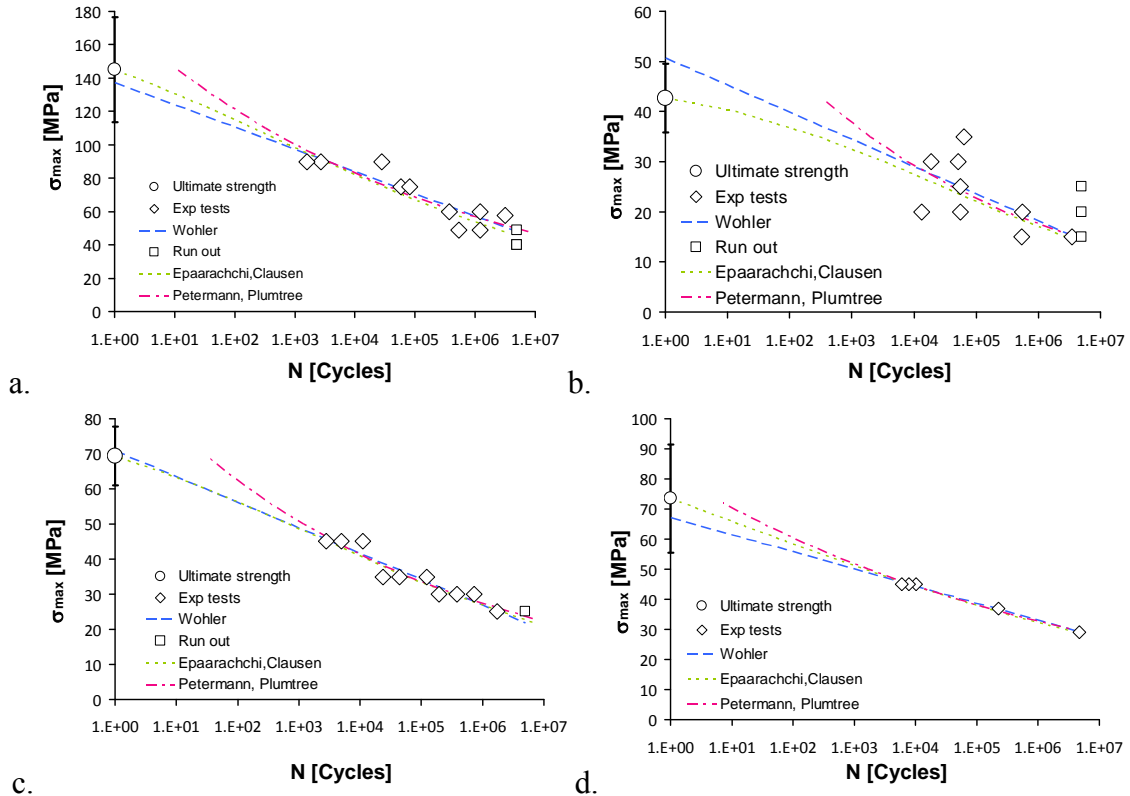


Figure 2. Results of the fatigue tests (a. L, b. N, c. I (45°) and d. I(30°) specimens).

From Eq. 2, and defining the damaging parameter  $D$  as:

$$D = \left( \frac{\sigma_u}{\sigma_{\max}} - 1 \right) \left( \frac{\sigma_u}{\sigma_{\max}} \right)^{0,6-\psi|\sin\theta|} \frac{1}{(1-\psi)^{1,6-\psi|\sin\theta|}} f^{\beta_1} \quad (3)$$

it is possible to estimate the fatigue life as:

$$D/\alpha_1 = (N^{\beta_1} - 1) \Rightarrow N = \beta_1 \sqrt{\frac{D}{\alpha_1} + 1} \quad (4)$$

The parameters  $\alpha_1$  and  $\beta_1$  required in the model can be estimated from the experimental fatigue data along the analyzed directions, by a regression and a further verification by means of residuals analysis.

The third applied criterion is the energetic model proposed by [11]. In this criterion, the strain energy density  $W^*$  can be evaluated from an extension of critical plane

concepts to unidirectional laminates. The multi-axial formulation is as a sum of the contribution of the normal stress and of the pure shear:

$$\begin{aligned}
 W_1^* &= \frac{1}{2}(\sigma_{22}^{\max} \epsilon_{22}^{\max} - \sigma_{22}^{\min} \epsilon_{22}^{\min}) = \frac{1}{2}(1-R^2) \sigma_{22}^{\max} \epsilon_{22}^{\max} = \frac{1}{2}(1-R^2) \frac{(\sigma_{22}^{\max})^2}{E_{22}} \\
 W_2^* &= \frac{1}{2}(\tau_{12}^{\max} \gamma_{12}^{\max} - \tau_{12}^{\min} \gamma_{12}^{\min}) = \frac{1}{2}(1-R^2) \tau_{12}^{\max} \gamma_{12}^{\max} = \frac{1}{2}(1-R^2) \frac{2(\tau_{12}^{\max})^2}{G_{12}} \\
 W^* &= W_1^* + W_2^*
 \end{aligned} \tag{5}$$

In Eq. 5, directions 1 and 2 are referred to a local coordinate system: direction 1 is along fibers while direction 2 is the in-plane one, perpendicular to fibers orientation.

If  $N$  specimens are considered, the contribution to the strain energy density  $W^*$  is only due to the first term,  $W_1^*$ . If  $I$  specimens are considered, on the contrary, both the contributions are present. The Peterman-Plumtree criterion proposes a linear regression in double logarithmic scale of  $W^*$  in function of  $N$ , number of loading cycles:

$$\text{Log}W^* = \beta_2 \text{Log}(N) + \alpha_2 \tag{6}$$

Once the constants  $\alpha_2$  and  $\beta_2$  fitted by the model are evaluated from the experimental data, it is possible to find the fatigue life estimation:

$$N = \beta_2 \sqrt{W^* \cdot 10^{-\alpha_2}} \tag{7}$$

In Fig. 2, the fatigue data are fitted by means of these three fatigue laws; considering their formulation, the only one, among these, interpolating the static ultimate strength is the Epaarachchi-Clausen [9, 10] criterion. This model appears therefore more precise with respect to the low fatigue cycling ( $N < 10^3$ ), where fatigue data have not been collected.

The Wöhler interpolation is, on the other side, a straight line. Its slope is highly dependent on the fatigue data, concentrated between  $10^3$  and  $5 \cdot 10^6$  cycles. When the estimation of fatigue life is extrapolated for  $N < 10^3$ , its reliability is lower. The same consideration is valid for the Petermann-Plumtree [11] interpolation. In Tab. 2 the coefficients interpolated from the fatigue experimental data of the specimens are indicated for the three criteria. The fit resulted fine for the  $L$  and  $I$  sets of specimens, while the statistic is less accurate for the  $N$  specimens, due to the high data dispersion. In Tab. 2 the coefficients are however indicated for a full comparison.

In order to have a complete comparison of the different sets of specimens and, therefore, directions of loading application to the composite material, a series of plots is presented in Fig. 3 and 4.

In Fig. 3.a the plot of the parameter  $D$  defined in Eq. 3, for the analyzed sets of specimens, is shown. This parameter has not an upper limitation (it is not normalized), but it has the meaning of the progressive damaging in the specimens. The trend is found

to be similar for all the four sets of specimens and the four curves fitting the experimental data are almost overlapping. This means that the global damage in the composite due to fatigue cycling can be described by the common parameter  $D$ : in Tab. 2, the estimated coefficients  $\alpha_1$  and  $\beta_1$  are indeed similar, especially for  $L$  and  $I(45^\circ)$  specimens.  $N$  specimens show slightly different values of  $\alpha_1$  and  $\beta_1$ , basically due to their high dispersion in the fatigue data, as already indicated.  $I(30^\circ)$  set shows different values of these parameters probably due to the small number of tested specimens.

Table 2. Coefficients of the fatigue models used for interpolating experimental data.

	<i>Specimen set</i>			
	$L$	$N$	$I(45^\circ)$	$I(30^\circ)$
$\alpha_0$	137.200	50.701	70.895	67.187
$\beta_0$	-13.333	-5.423	-7.334	-5.692
$\alpha_1$	0.362	0.186	0.355	0.557
$\beta_1$	0.206	0.253	0.203	0.143
$\alpha_2$	0.127	-0.076	-0.110	-0.134
$\beta_2$	-0.165	-0.222	-0.180	-0.481

In Fig. 3.b the trend of the strain energy density, as calculated from Eq. 5, is plotted. A regression linear line is plotted in the double log graph of Fig. 3.b, for the  $N$  and  $I$  specimens. These data seem pretty aligned on this trend.

In the light of a comparison with a previous study [12], where other fatigue experimental tests were described, a set of plots is shown in Fig. 4. The composite material [12] is characterized by higher values of the global mechanical properties, if compared to the ones in the present work. The comparison is therefore performed by means of a normalization of the stress with respect to the ultimate static strength,  $\sigma_{\max}/\sigma_u$ . In Fig. 4.a all the experimental fatigue data are plotted.

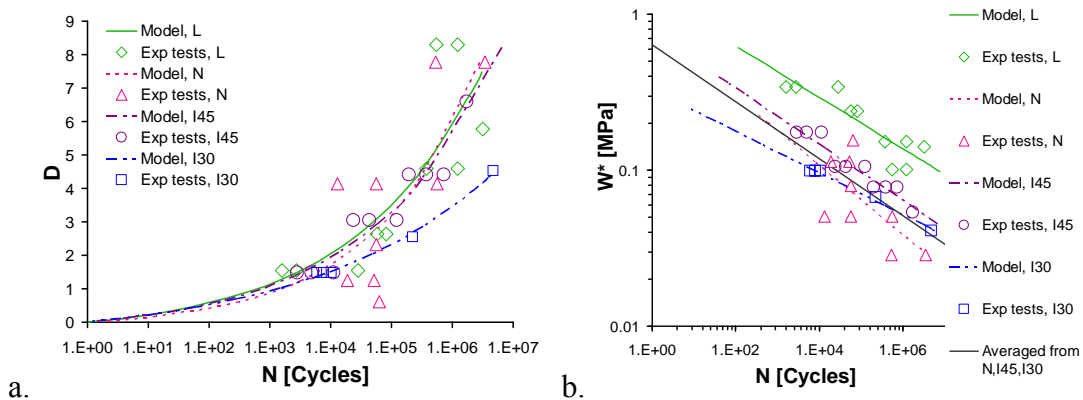


Figure 3. Evaluation of the damage parameters according to a. [9] and b. [11].

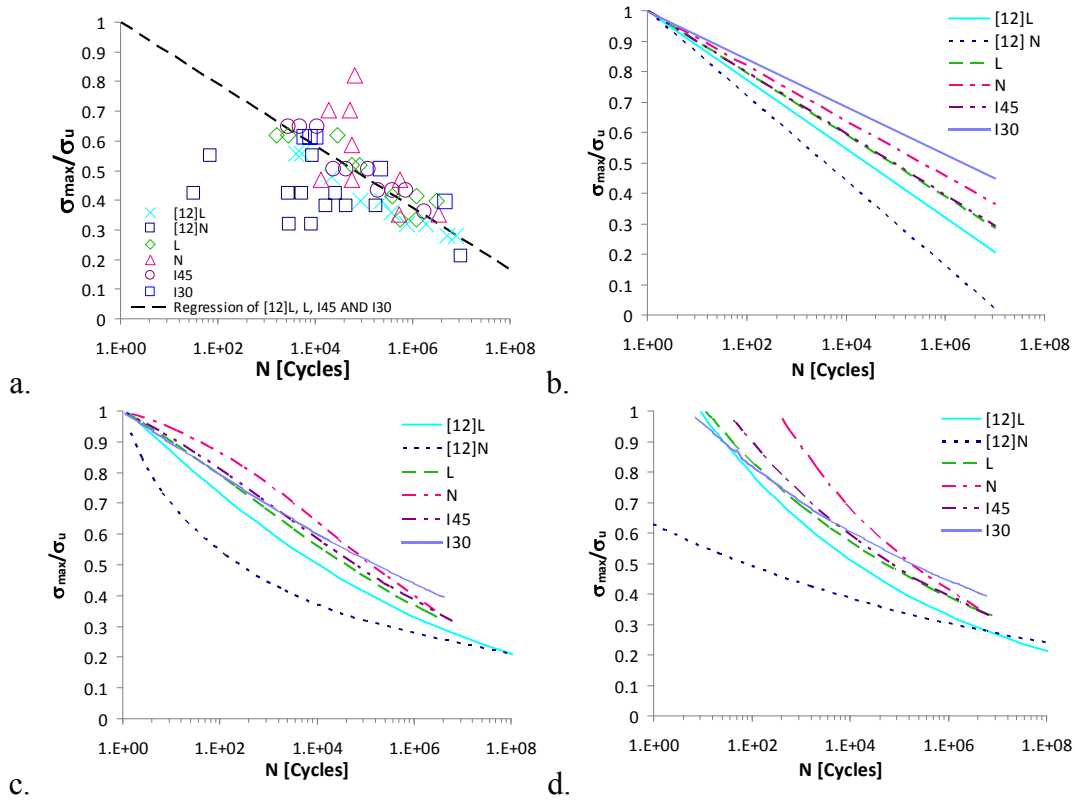


Figure 4: Comparison between the present work material and the one analysed in [12]: experimental data (a.) and their interpolation by eq.1 (b.), eq.4 (c.) and eq.7 (d.).

Considering Eq. 1, the Wöhler model, the interpolation is forced to pass from  $\sigma_{\max}/\sigma_u = 1$ , the average ultimate strength value. From the regressions, it is possible to observe that, if the normal specimens of both the sections are excluded due to the high dispersion along the normal direction, the straight lines of  $L$  and  $I$  specimens are very similar and next to the line fitting the longitudinal data of [12]. This indicates that the progressive decreasing of the mechanical properties during fatigue is similar for the two materials, one described in [12] and one described in the present work. In particular, although the mechanical properties are higher for the material described in [12], the behavior is the same of present work material, in the  $\sigma_{\max}/\sigma_u - \log N$  plot. This is a useful consideration to understand and evaluate the fatigue behavior of composites from the only static characterization.

Besides, the same considerations result valid for composites characterized by different angles between the fibers and the load application direction. In this light, a straight line is plotted in the graph of Fig. 4.a, corresponding to the regression fitted on the  $L$  and  $I$  specimens. This line has the following equation:

$$\frac{\sigma_{\max}}{\sigma_u} = -0.1043 \cdot \log N + 1 \quad (8)$$

This can summarize the fatigue behavior of this kind of composites (E-glass and vinyl-ester), in terms of  $S-N$  curves.

In Fig. 4.c the interpolation of the fatigue data by means of Eq. 4, the Epaarachchi-Clausen model, is presented. Curves are all starting from  $\sigma_{\max}/\sigma_u = 1$  since the static ultimate strength is interpolated by this model. In Fig. 4.d the experimental data are interpolated by means of Eq. 7, the Peterman-Plumtree model. In both these plots, the same considerations presented for Fig. 3.a are valid.

These three criteria, in conclusion, agree for both the materials, described in the present work and in [12], and for all the specimens with different inclination fibers-load application direction.

## 5. CONCLUSIONS

In the present work, a series of experimental tests was described, to obtain the mechanical characteristics of a composite material made by the pultrusion technique. The composite is reinforced by E-glass fibers, and the matrix is vinyl-ester. This material is used in the manufacturing of a corner beam to be placed in a cabin bus, designed with innovative concepts. In conclusion the following points are evidenced:

- specimens were extracted from the component, with four different fibers inclinations. Experimental static and fatigue tests were carried out to understand the mechanical behavior of the composite material;
- the fatigue data were interpolated by means of three different fatigue laws: these models showed a good data fitting and all agree in the estimation of fatigue life;
- in order to offer a more general assessment about this material, unified fatigue parameters are calculated,  $D$  according to [9] and  $W^*$  according to [11];
- a comparison with a previous work fatigue tests was presented. Considering the normalization of the mechanical properties with respect to the static ultimate strength, common fitting trends of the considered criteria were found.

## REFERENCES

1. <http://www.litebus.com/>
2. Degriek, J. and Van Paepegem, W. (2001) *Appl. Mech. Reviews*, **54**: 279-300.
3. Harris, B. (2003). *Fatigue in Composites, Part 1: A historical review of the fatigue behaviour of fibre-reinforced plastics*. Woodhead Publishing Lim., Abington Hall, Cambridge, UK.
4. Gude, M., Hufenbach, W., Koch, I., and Protz, R. (2006) *Mech. Comp. Mat.*, **42**: 443-450.
5. McCartney, L.N. (2008) *Comp. Sci. Tech.*, **68**: 2601-2615.
6. Revuelta, D. and Miravete, A. (2002) *Intl. Appl. Mech.*, **38**: 121-134.
7. Hashin, Z., and Rotem, A. (1973) *J. Comp. Mat.*, **7**: 448-464.
8. Quaresimin, M., Susmel, L. and Talreja R. (2010) *Int. J. Fatigue*, **32**: 2-16.
9. Epaarachchi, J. A. and Clausen, P. D. (2003) *Composites A*, **34**: 313-326.
10. Caprino, G. and D'Amore, A. (1998) *Comp. Sci. Tech.*, **58**: 957-965.
11. Petermann, J. and Plumtree, A. (2001) *Composites A*, **32**: 107-118.
12. Colombo, C. and Vergani L. (2010) *Comp. Struct.*, **92**: 1706-1715.